Atmos. Chem. Phys., 8, 2933–2948, 2008
www.atmos-chem-phys.net/8/2933/2008/

Atmospheric Chemistry and Physics

Cloud condensation nuclei activity at Jeju Island, Korea in spring 2005

M. Kuwata[1], Y. Kondo[1], Y. Miyazaki[1,*], Y. Komazaki[1], J. H. Kim[2], S. S. Yum[2], H. Tanimoto[3], and H. Matsueda[4]

[1]Research Center for Advanced Science and Technology, the University of Tokyo, Tokyo, Japan
[2]Department of Atmospheric Science, Yonsei University, Seoul, Korea
[3]Atmospheric Environmental Division, National Institute for Environmental Studies, Tsukuba, Japan
[4]Geochemical Research Department, Meteorological Research Institute, Tsukuba, Japan
[*]now at: Institute of Low Temperature Science, Hokkaido University, Japan

Received: 12 October 2007 – Published in Atmos. Chem. Phys. Discuss.: 13 November 2007
Revised: 14 May 2008 – Accepted: 14 May 2008 – Published: 11 June 2008

Abstract. We measured the number concentrations of cloud condensation nuclei (CCN) and the size distributions of CCN/CN (CN: condensation nuclei) ratios at supersaturations (SSs) of 0.097, 0.27, 0.58, and 0.97% at Jeju Island, Korea during March-April 2005. We made simultaneous measurements of aerosol inorganic ions, water-soluble organic carbon (WSOC), organic carbon (OC), and elemental carbon (EC) in $PM_{2.5}$. The CCN/CN ratios increased with increasing particle diameter, and the diameter at CCN/CN=0.5 was defined as D_{50}. D_{50} represents the activation dry diameter of atmospheric particles. The average D_{50} at SS=0.097% and 0.97% was 136±17 nm and 31±3 nm, respectively. The temporal variation of D_{50} at SS=0.097% was correlated with the mass fraction of water-soluble components (inorganic ions + WSOC), indicating that the temporal variation of CCN activity was mainly controlled by changes in the water-soluble components fraction. The critical dry diameter (D_{crit}), which is the threshold dry diameter for CCN activation, was calculated from the observed aerosol chemical compositions by Köhler theory for comparison with D_{50}. The D_{50} at SS=0.097% was correlated (r^2=0.48) with calculated D_{crit}, although D_{crit} was larger than D_{50} by 20–29% on average. The systematic difference between D_{50} and D_{crit} could be caused by the size dependence of the aerosol chemical compositions or surface tension lowering caused by the mixing of water-soluble organic compounds. This difference corresponds to a 27±14% uncertainty in the CCN number concentration estimated from the observed particle number size distribution.

Correspondence to: Mikinori Kuwata
(kuwata@atmos.rcast.u-tokyo.ac.jp)

1 Introduction

A subset of atmospheric particles acts as cloud condensation nuclei (CCN). An increase in CCN number concentration causes an increase in cloud droplet concentration and a decrease in droplet size, which in turn impacts cloud albedo and precipitation. Consequently, CCN can significantly influence climate through cloud processes (Twomey, 1974; Lohmann and Feichter, 2005, and references therein).

The number concentration of CCN is determined by the number concentration of aerosol particles and the fraction of CCN active particles. This fraction is often denoted as the CCN/CN ratio because condensation nuclei (CN) counters have been used for total particle number concentration measurements (Seinfeld and Pandis, 2006). CCN/CN strongly depends on the size and chemical composition of aerosols. The influence of aerosol chemical composition and number size distribution on the bulk (size-unresolved) CCN/CN can be separated by measuring CCN/CN for size-selected particles. In particular, when aerosol particles are internally mixed, we can determine the threshold diameter from the measurements (Dusek et al., 2006). The threshold diameter can also be calculated by Köhler theory. Many laboratory studies have measured CCN/CN ratios of size-selected particles for comparison with theoretical calculations (e.g. Corrigan and Novakov, 1999; Raymond and Pandis, 2002). These experiments have shown that size-resolved CCN/CN ratios of laboratory-generated particles can be explained by Köhler theory. However, only a few studies have employed this measurement method for atmospheric observations (e.g. Dusek et al., 2006), leading to an insufficient understanding of controlling factors for the CCN activation of atmospheric particles.

Published by Copernicus Publications on behalf of the European Geosciences Union.

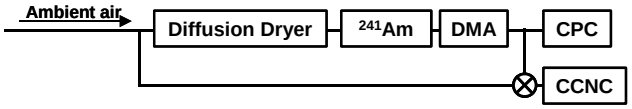

Fig. 1. CCN observation system used for this study. The three-way valve placed upstream of the CCN counter was used to select the sampling mode (see text for detailed explanation).

CCN concentrations are often influenced by anthropogenic particles (Twomey, 1974; Hudson and Yum, 2002). In recent years, anthropogenic emission of aerosol precursors (e.g. SO_2 and NO_x) from Asia has increased significantly (Streets et al., 2000; Akimoto et al., 2003; Richter et al., 2005). Remote sensing studies have indicated that the aerosol particles derived from anthropogenic pollutants from Asia have changed cloud radiative properties such as optical depth in this region (Chameides et al., 2002; Kawamoto et al., 2006). Thus, it is important to study CCN activity in this region for a more accurate assessment of the impact of anthropogenic aerosol on climate. However, only a few CCN studies have been performed in this region (e.g. Matsumoto et al., 1997; Yum et al., 2005), and the size-resolved CCN/CN ratios have not been measured so far.

In this study, we have measured size-resolved CCN/CN ratios and CCN number concentrations at Gosan, Jeju Island, Korea, in March and April 2005 during the United Nations Environmental Programme (UNEP) Atmospheric Brown Cloud – East Asian Regional Experiment 2005 (ABC-EAREX2005) campaign. In addition to the CCN measurements, aerosol chemical composition was simultaneously observed. Observed threshold diameters for CCN activation are compared with the mass fractions of aerosol chemical compositions. Threshold diameters for activation (D_{crit}) are calculated and compared with the observed threshold diameter to investigate the controlling factors of D_{crit}.

2 Theory

The equilibrium water vapor pressure (S) of an aerosol particle can be calculated by Köhler theory. According to the theory, S is described as follows (e.g. Roberts et al., 2002; Mochida et al., 2006):

$$\ln S = \frac{A}{d_{\mathrm{wet}}} - \frac{B d_{\mathrm{dry}}^3}{(d_{\mathrm{wet}}^3 - d_{\mathrm{dry}}^3)} \left(A = \frac{4 M_w \sigma}{RT\rho_w} \quad B = \frac{M_w}{\rho_w} \frac{\sum_i \frac{v_i \phi_i \varepsilon_i m_i}{M_i}}{\sum_i \frac{m_i}{\rho_i}} \right) \tag{1}$$

where d_{dry} is the dry diameter of a particle and d_{wet} is the diameter of a droplet under equilibrium conditions. The suffix i denotes the properties of the i-th solute compound. M_w is the molecular weight of water; M_i is the molecular weight of solute; ρ_w is the density of water; ρ_i is density of solute; σ is the surface tension; R is the gas constant; T is the temperature; v_i is the stoichiometric number of ions and molecule; ϕ_i is the osmotic coefficient; ε_i is the degree of dissolution; and m_i is the mass mixing ratio of the i-th solute. The first term on the right-hand side represents an increase in the equilibrium vapor pressure of water due to surface tension (the Kelvin effect). The second term on the right-hand side denotes the decrease in the equilibrium vapor pressure of water because of solute mixing (Raoult's effect). When we consider S for an aerosol particle, it has a maximum value at a certain d_{wet} (critical droplet diameter). The supersaturation (SS: SS=$S-1$) that corresponds to this S is called the critical supersaturation (SS_c). Particles can be activated to cloud droplets if the SS of the environment is higher than their SS_c.

If we assume that A and B are constants and d_{wet} is much larger than d_{dry}, SS_c can be expressed as follows:

$$\ln(1 + SS_c) = \sqrt{\frac{4A^3}{27 B d_{\mathrm{dry}}^3}}. \tag{2}$$

This equation shows that SSc decreases with particle diameter. Thus, at a certain SS, there exists a threshold value of d_{dry} above which all aerosol particles act as CCN. We denote this diameter as the critical dry diameter (D_{crit}).

3 Experiment

3.1 CCN measurement

Figure 1 shows the CCN observation system used for this study. In this system, the relative humidity of the sample flow was reduced using two diffusion dryers in series (TSI Model 3062). Silica gel was replaced periodically (about 1 time in 10 days), and no systematic change in size-resolved CCN spectra was observed before or after the replacement. Then, particles were charged with a ^{241}Am bipolar neutralizer and introduced to a differential mobility analyzer (DMA: TSI Model 3081). The DMA classified particles by their electrical mobility. The voltage applied to the DMA was scanned stepwise to change the diameter of the classified particle (Table 1). The sheath to-sample flow ratio of the DMA was set to 10:1. Classified particles were introduced to a condensation particle counter (CPC: TSI Model 3022) and a cloud condensation nuclei counter (CCNC: Droplet Measurement Technologies, Inc.) (Roberts and Nenes, 2005). The CPC monitored the number concentrations of condensation nuclei (CN), and the CCNC measured number concentrations of CCN. The sample flow rate of the CCNC was set to 0.045 l/min, and the sheath flow rate was set to 0.455 l/min. The temperature gradient (ΔT) of the thermal gradient chamber in the CCNC was changed periodically to alter the SS in the chamber. Four ΔTs (3.08, 4.62, 9.24, and 15.4 K) were used in this study. SSs corresponding to these ΔTs were calibrated with ammonium sulfate particles

Table 1. Calibration results and operating conditions of the CCN measurement system shown in Fig. 1. SS was calculated at 300 K and 72 mN/m by the ideal solution approximation. The values in parentheses show SS calculated using the osmotic coefficient of Clegg et al. (1996).

ΔT(K)	Activation dry diameter of $(NH_4)_2SO_4$(nm)	SS (%)	Particle diameters classified by the DMA(nm)
3.08	125±3	0.097(0.10)	80, 100, 110, 120, 130, 140, 160, 180, 200, 240, 290
4.62	63±2	0.27(0.30)	60, 65, 70, 75, 80, 85, 90, 100, 130, 160, 200, 240, 290
9.24	38±1	0.58(0.65)	35, 40, 45, 50, 60, 70, 80, 100, 130, 160, 200, 240, 290
15.4	27±1	0.97(1.1)	25, 30, 35, 40, 50, 60, 80, 100, 130, 160, 200, 240, 290

as described by Kuwata et al. (2007). The calibration was performed at the observation site before and after the campaign. There are several different methods for the calculation of the water activity of ammonium sulfate particles (Kreidenweis et al., 2005, and references therein). We chose the ideal solution approximation (ϕ=1) in calculating the D_{crit} of atmospheric particles (Sect. 5). Therefore we used this approximation for the interpretation of the calibration results to ensure consistency, although SSs calculated using the osmotic coefficient of Clegg et al. (1996) are likely to be more plausible than the ideal solution approximation, as it is based on precise experimental data. We also show SSs calculated using the osmotic coefficients by Clegg et al. (1996) for reference in parentheses in Table 1. The Debye – Hückel constant is needed to calculate the osmotic coefficient of Clegg et al. (1996) because it is based on the Pitzer model. The Debye – Hückel constant at 300 K was calculated by the equation given by Clegg et al. (1994).

Multiply charged particles were included in the classified particles, therefore an inverse analysis was performed for CCN and CN size distribution data for multiple-charge correction. The STWOM algorithm (Markowski, 1987) was used to obtain size distributions of CN and CCN. In this calculation, the equilibrium charge distribution (Wiedensohler, 1988) and the DMA transfer function derived by Knutson and Whitby (1975) were included in the kernel function. The raw data for CN and CCN were linearly interpolated so that the interval of each bin was $\Delta \log d_p$=0.015. Size-resolved CCN/CN ratios were calculated using the data after the inverse analysis.

The three-way valve in Fig. 1 was switched once every 30 min for the direct measurement of the CCN number concentration in ambient air. It took 30 min for the measurement at each SS, and 2 h were required for the entire measurement cycle.

3.2 Measurements of aerosol composition, size distribution

Inorganic components (NH_4^+, Na^+, K^+, Ca^{2+}, Mg^{2+}, NO_3^-, SO_4^{2-}, Cl^-) were measured by a particle-into-liquid sampler combined with ion chromatography (PILS-IC) (Orsini et al., 2003; Takegawa et al., 2005). The concentration of water-soluble organic carbon (WSOC) was measured by PILS combined with a total organic carbon analyzer (PILS-WSOC) (Sullivan et al., 2004; Miyazaki et al., 2006, 2007). Elemental carbon (EC) and organic carbon (OC) were measured by a semi-continuous thermal-optical carbon aerosol analyzer (Sunset Laboratory, Inc.) (Bae et al., 2004; Kondo et al., 2006; Miyazaki et al., 2006). $PM_{2.5}$ cyclones were used for these instruments. The detection limits of the PILS-IC, PILS-WSOC, OC, and EC were estimated to be 0.01 μg/m^3, 0.1 μg/m^3, 1.0 μg/m^3, and 0.2 μg/m^3, respectively (Takegawa et al., 2005; Kondo et al., 2006; Miyazaki et al., 2006).

Aerosol number size distribution (10–300 nm) was measured with a scanning mobility particle sizer (SMPS 3936, TSI). The SMPS used in this study comprised a DMA (TSI Model 3081) and a CPC (TSI Model 3010). In addition, the number concentration of particles larger than 10 nm (CN) was measured by another CPC (TSI Model 3010) (Yum et al., 2007). The concentration of carbon monoxide (CO) was measured using a non-dispersive infrared analyzer (Horiba APMA-360 model) (Tanimoto et al., 2007).

3.3 Measurement site

The observations were performed between 18 March and 5 April 2005 at Gosan (33.2° N, 126.1° E) on Jeju Island, Korea, as part of the Atmospheric Brown Cloud – East Asian Regional Experiment 2005 campaign. The location of Gosan is shown in Fig. 2. The instruments were placed in a container located about 10 m back from the edge of a cliff. The sampling inlets were made of stainless steel tubes with an inner diameter of 7 mm. The top of the inlets was located about 4 m a.g.l.

The meteorological parameters at the Gosan site were observed by the Korean Meteorological Administration (KMA). During the observation period, the dominant winds were northerlies and north-northwesterlies (more than 50% of the observation period) associated with the Siberian high-pressure system. This led to the frequent transport of anthropogenic pollutants from the Korean Peninsula and China to Gosan. Sawa et al. (2007) attributed the high concentrations of CO at Gosan to the emissions from these regions based

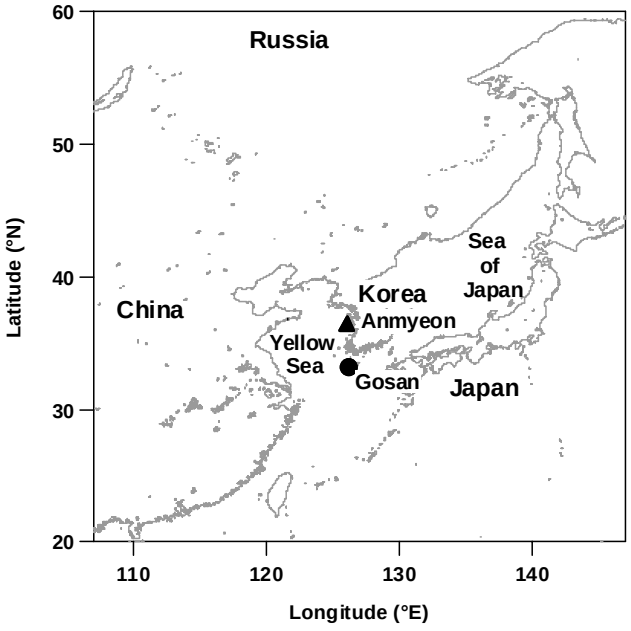

Fig. 2. Map of Gosan and surrounding region.

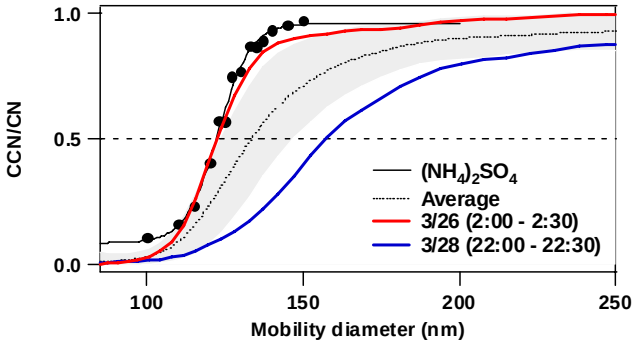

Fig. 3. Size distributions of CCN/CN ratios of ammonium sulfate and atmospheric particles at SS=0.097%. The average, standard deviation (gray area), and two examples of CCN/CN during the observation period are shown. The solid circles denote the experimental data for ammonium sulfate under the observation conditions and the solid line shows the fitting results of the experimental data.

on tagged CO-tracer simulations. More detailed descriptions of the meteorological conditions and the transport of anthropogenic pollutants can be found elsewhere (Sawa et al., 2007; Miyazaki et al., 2007). Previous studies have also shown that air masses observed at Gosan are heavily influenced by anthropogenic emissions from East Asia (Carmichael et al., 1997; Lee et al., 2006).

4 Results

4.1 CCN/CN size distributions

Figure 3 shows the average size-resolved CCN/CN ratio at SS=0.097%, together with the data on specific days. The CCN/CN size distribution of ammonium sulfate obtained during calibration at the observation site (closed circles) is also shown in this figure for comparison. In general, CCN/CN increases with increasing diameter. At 02:00–02:30 on 26 March, the CCN/CN size distribution of ambient particles was very similar to that of ammonium sulfate. On the other hand, on 28 March, the CCN/CN size distribution shifted to a larger diameter, and the rate of increase was lower than ammonium sulfate. In addition, the spectrum is significantly different from a sigmoid function. This shift indicates that the bulk aerosol chemical composition on 28 March was significantly different from ammonium sulfate. The slower rate of increase indicates the co-existence of different types of aerosol particles with different activation curves. A convolution of sigmoid functions is not necessarily a sigmoid function. Thus, the non-sigmoid shape of the spectrum can be interpreted as a result of the co-existence of different types of aerosol particles. The different width of the DMA transfer function at D_{50} in diameter space (∼25%: estimated by a Knutson-type DMA transfer function) is not large enough to explain the lower increase rate, as the widths of the activation curves are different by about a factor of 2.

We defined the threshold diameter for CCN activation to compare it with the mass fraction of chemical compounds and theoretically calculated D_{crit}. In this study, the threshold diameter was defined as the diameter corresponding to CCN/CN=0.5(D_{50}) because it represents the bulk chemical composition. If aerosol particles were not fully activated, D_{50} would not necessarily correspond to the threshold diameter. In all cases shown in Fig. 3, the CCN/CN ratios exceeded 0.85 at 250 nm. In addition, no multi-step activation was observed. These results suggest the appropriateness of the definition of the unique activation diameter (D_{50}). Previous studies on CCN activity of laboratory-generated particles have shown that D_{50} can be quantitatively compared with the theoretically calculated activation diameters (e.g. Corrigan and Novakov, 1999; Raymond and Pandis, 2002).

4.2 Temporal variation of CCN and particle number size distribution

4.2.1 CCN number concentration

Figure 4a shows the time series of the CCN number concentration. In general, the variation in the CCN number concentration was correlated with that of CO concentration (Fig. 4d). In particular, this correlation is clearly observed at SS=0.097% (r^2=0.74). Sawa et al. (2007) have reported high CO concentration between 22–24 March and 30 March–2 April due to transport of CO from the Korean Peninsula and China. During these periods, CCN concentration also increased (Fig. 4a and d). CO is emitted mainly by the incomplete combustion of fossil fuels and biomass, and it is a

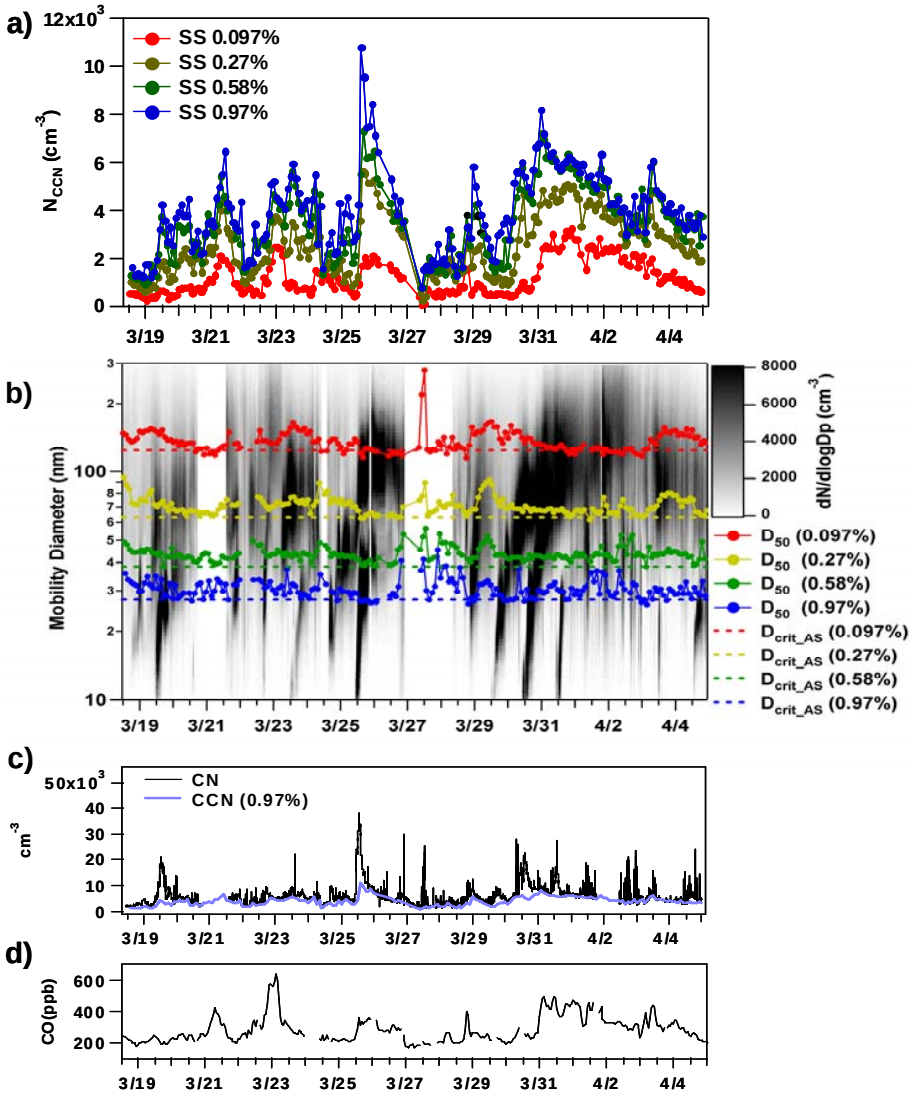

Fig. 4. Time series of **(a)** CCN number concentration, **(b)** aerosol size distribution, D_{50}, **(c)** CN concentration, CCN (SS=0.97%) concentration, and **(d)** CO concentration. The dashed lines in (b) shows the D_{crit} of ammonium sulfate at each SS.

good indicator of emissions from combustion sources. Primary aerosols and aerosol precursors such as SO_2 and NO_x are co-emitted with CO. Thus, these high CCN concentrations were likely caused by the enhanced concentrations of anthropogenic aerosols transported from these regions. The average values and standard deviations of CCN number concentration are shown in Table 2. The average CCN number concentration at SS=0.097% and 0.97% was 1200 cm^{-3} and 4000 cm^{-3}, respectively. These concentrations are higher than those of other remote areas of the world such as the Island of Tasmania in Australia and Mace Head in Ireland by about an order of magnitude (Covert et al., 1998; Reade et al., 2006). CCN concentrations measured at Gosan during this observation period were extensively compared with those obtained in other regions by Yum et al. (2007). The CCN concentrations observed in this study are close to those of Anmyeon (Korea: see Fig. 2) in springtime of 2004 (SS=1%) (Yum et al., 2005).

4.2.2 D_{50}

Figure 4b shows the time series of the number size distribution of aerosol particles and D_{50}. The D_{crit} of ammonium sulfate at each SS is also shown as dashed lines in this figure. The average values of D_{50} at SS=0.097% and 0.97% were 136 nm and 31 nm, respectively (Table 2). In general, the D_{50} is almost equal to or slightly larger (by ~25%) than the D_{crit} of ammonium sulfate (125 nm and 27 nm, respectively). This means that the D_{crit} of ammonium sulfate is the smallest D_{crit} of the atmospheric particles during the observation period.

Table 2. Average values and standard deviations of the CCN number concentration, D_{50}, and B. The surface tension of water was assumed for the calculation of B.

SS (%)	CCN number concentration (cm^{-3})	D_{50} (nm)	B
0.097	1194 ±746	136±17	0.61±0.17
0.27	2543 ±1277	71±6	0.55±0.12
0.58	3496 ±1510	44±3	0.50±0.09
0.97	3996 ±1686	31±3	0.55±0.13

The temporal variation of D_{50} at different SSs did not always correlate. As shown in Eq. (2), the threshold diameter for CCN activation depends on A and B, which are determined by the aerosol chemical composition. Thus, this difference in the temporal variations of D_{50} at each SS indicates the difference in temporal variation of chemical composition in different size ranges.

Using Eq. (2), we calculated B assuming the surface tension of water. This parameter gives information on the chemical composition (approximate number of solute ions and molecules included in a unit volume) at D_{50} for each SS. The results are summarized in Table 2. The average values of B did not depend on SS significantly, indicating that the chemical composition averaged over the observation period was rather uniform in the diameter range considered (30 to 160 nm).

4.2.3 Number size distribution

New particle formation events can have a significant impact on CCN number concentration (e.g. O'Dowd et al., 2002; Laaksonen et al., 2005). In Fig. 4b, new particle formation is clearly identified on 19, 25, 29, 30 and 31 March. It can be seen more clearly in Fig .4c, which shows the particle number concentration measured by CPC and CCN number concentration (SS=0.97%). The concentration of CCN (SS=0.97%) is a good indicator of particle number concentrations larger than 30 nm, as the average value of D_{50} at SS=0.97% is 31±3 nm (Table 2). Thus, the difference of the number concentrations (CN-CCN (SS=0.97%)) represents the number concentration of particles between 10 and 30 nm. During the periods of new particle formation events described above, an enhancement of the number concentration of small (10–30 nm) particles was observed, as indicated by the large gap between CN and CCN concentrations. In particular, the events occurring on 29 and 30 March were important in that newly formed particles influenced the CCN number concentration as a consequence of particle growth beyond D_{50}. Figure 5a and b shows the CCN number concentrations, particle size distributions, and D_{50} during this event. The peak diameter of the size distribution obtained by bimodal lognormal fitting is shown as red lines in Fig. 5b.

At 14:00 local time (LT) on 29 March, small (<20-nm) particles appeared and began to grow. The peak diameter grew to 25 nm by 18:00 LT, and some particles grew larger than the D_{50} at SS=0.97% (28 nm). At this time, the CCN number concentration (SS=0.97%) began to increase. The peak diameter and D_{50} (SS=0.97%) were equal at 21:00 LT (blue dashed vertical line in Fig. 5b). At this time, the majority of newly formed particles began to act as CCN at SS=0.97%. In the case of SS=0.58%, the peak diameter equaled D_{50} at 2:00 LT on 30 March , and the CCN number concentration increased from 1700 cm^{-3} (01:30 LT) to 5800 cm^{-3} (11:30LT). At 03:00 LT, some portion of the particles grew large enough to act as CCN at SS=0.27%. Then, CCN number concentration at SS=0.27% increased from 1000 to 4700 cm^{-3} with the increase in the peak diameter. For this SS, the peak diameter reached D_{50} at 10:00 LT. At the same time, another new particle formation event occurred, and this event also clearly affected the CCN number concentration at SS=0.97% and 0.58%. At 12:00 LT, some fraction of the particles grew larger than the D_{50} at SS=0.097%, and they affected the CCN number concentration at this SS. A similar phenomenon was also observed on 25 March (Fig. 4a and b). These results clearly show that the newly formed particles significantly increased the CCN number concentration.

Buzorius et al. (2004) have shown that the deliquescence relative humidity and the hygroscopic growth of newly formed particles at Gosan during the ACE-Asia campaign were similar to those of ammonium sulfate. This suggests that newly formed particles were mainly composed of inorganic compounds because no organic compounds in the atmosphere are known to be as hygroscopic as ammonium sulfate. In addition, according to Buzorius et al. (2004), glutaric acid is the only organic compound that is known to have a deliquescence relative humidity similar to ammonium sulfate. However, the hygroscopic growth of glutaric acid is less than ammonium sulfate. For instance, Cruz and Pandis (2000) measured the hygroscopic growth factors of glutaric acid and ammonium sulfate particles to be 1.1 and 1.5 at a relative humidity of 85%, respectively. This also supports the conclusion of their study that newly formed particles were mainly composed of ammonium sulfate at Gosan. In the present study, the observed D_{50} of newly formed particles

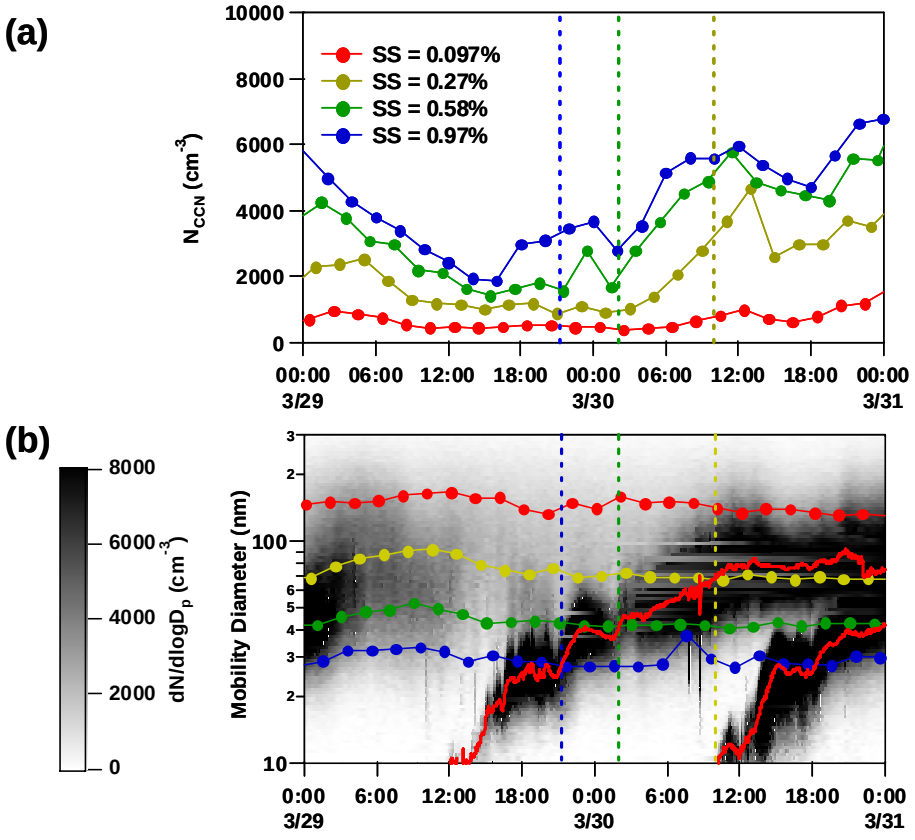

Fig. 5. Close-up of Fig. 4 during the new particle formation events from 29–31 March. The **(a)** time series of CCN number concentration and **(b)** the number size distribution and D_{50} (line with filled circles) are shown. The red solid lines in (b) denote the peak diameters obtained by bimodal lognormal fitting. The vertical dashed lines show the time at which the peak diameter and D_{50} were equal.

was also similar to ammonium sulfate. For instance, the D_{50} for SS=0.97% was 27 nm at 21:00 LT, 29 March, and for SS=0.27% it was 66 nm at 10:00 LT, 30 March. The D_{crit} of ammonium sulfate was 27 nm and 63 nm, respectively (Table 1).

Previous studies have suggested that new particle formation has an impact on the CCN number concentration from the measurements of number size distributions (e.g. O'Dowd et al., 2002; Laaksonen et al., 2005) and modeling (e.g. Arnold, 2006; Sotiropoulou et al., 2006). The present observations clearly demonstrate that new particle formation is one of the important processes of CCN formation at Gosan.

Figure 6 shows the number size distribution of all particles and CCN averaged over the whole observation period. Average CCN/CN ratios were multiplied by the number size distribution measured by the SMPS averaged over the observation period to obtain a rough estimate of the CCN size distribution. The peak diameter of the average CCN size distribution was about 150 nm at SS=0.097% and shifted to about 80 nm at SS=0.97%. Detailed discussion of the number size distribution of particles during the observation period has been given by Yum et al. (2007).

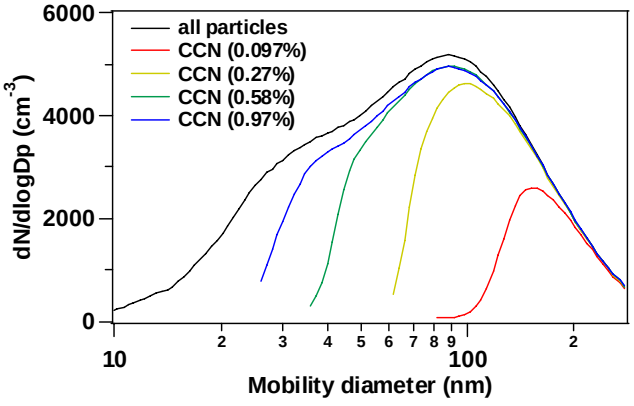

Fig. 6. Number size distribution of particles and CCN. CCN size distributions were estimated by multiplying CCN/CN ratios by the number size distribution. The data were averaged over the whole observation period. The data range of CCN size distributions was limited by the scanning range of the DMA.

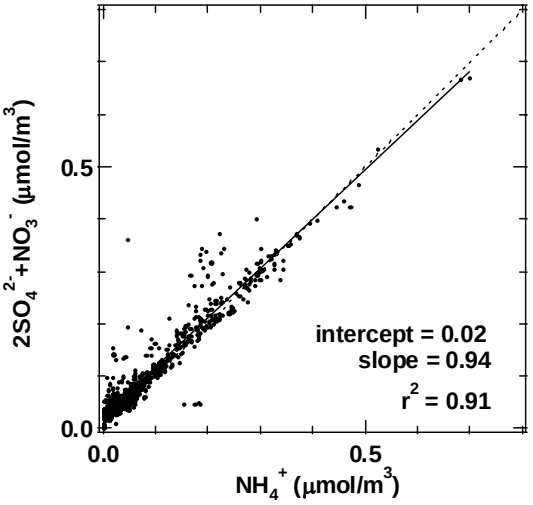

Fig. 7. Ion balance between ammonium, sulfate, and nitrate ions.

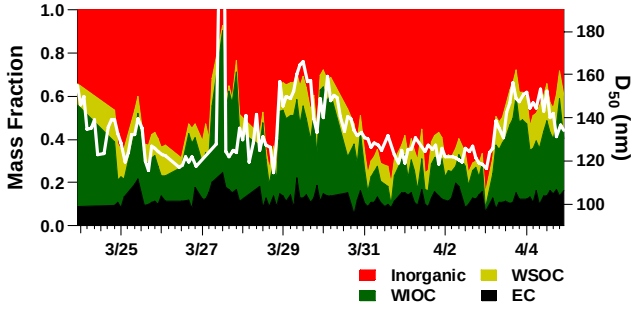

Fig. 8. Temporal variation of the mass fraction of aerosol components and D_{50} at SS=0.097%. Here, "inorganic" denotes the sum of ammonium sulfate and ammonium nitrate.

4.3 Ion balance of inorganic components

The average concentrations of the inorganic components measured by PILS-IC are summarized in Table 3. NH_4^+ was the most abundant cation (56%), and Ca^{2+} was the second (15%). SO_4^{2-} was the most abundant anion (67%). Topping et al. (2004) measured inorganic components using a Berner impactor at Gosan during the ACE-Asia campaign. They showed that the concentration of NH_4^+ was the highest at the 0.2–0.5 μm stage, and Ca^{2+} was the highest at the 1.5–5.5 μm stage. In this study, the D_{50} values were in the sub-micrometer range (Fig. 4). Thus, Ca^{2+} was ignored in the following discussion of CCN activity. Na^+, Mg^{2+}, and Cl^- were also ignored for the same reason.

Figure 7 shows the ion balance of NH_4^+, NO_3^-, and SO_4^{2-}. The cation and anions balance very well (slope=0.94). This result shows that sulfate and nitrate in $PM_{2.5}$ were neutralized by ammonium at Gosan. The addition of K^+ to the ion balance causes the balance to deviate from the 1:1 line. This suggests that neither NO_3^- nor SO_4^{2-} were the counter ions of K^+. In addition, because the molar concentration of K^+ was only 8% of NH_4^+, we ignored K^+. In the following discussion, we assume that the inorganic component of sub-micron particles was composed only of ammonium sulfate and ammonium nitrate.

5 Discussion

5.1 Temporal variation of D_{50} and aerosol composition

Figure 8 shows the temporal variation of D_{50} (SS=0.097%) and the mass fraction of the aerosol components. In this figure, the aerosol components were divided into four groups: inorganic (NH_4^+ + SO_4^{2-} + NO_3^-), WSOC, water-insoluble organic carbon (WIOC = OC – WSOC), and EC. Inorganic components and WSOC are soluble in water, while WIOC and EC are insoluble in water. Note that the masses of WSOC and WIOC are the masses of carbon in organic compounds and do not include the masses of other elements (e.g. oxygen and hydrogen) (Kondo et al., 2007). The temporal variation of D_{50} and the water-soluble fraction (inorganic + WSOC) are correlated. With an increase in the water-soluble fraction, D_{50} decreases. This is consistent with Köhler theory because the value of B in Eq. (2) increases with an increase in the water-soluble fraction. In this case, the variation in D_{50} was as small as about 40 nm. Thus, D_{50} is correlated with the water-soluble fraction almost linearly, although the relationship is not always linear, as anticipated from Eqs. (1) and (2). This good correlation indicates that the variation of D_{50} was not significantly influenced by the variation in the chemical composition of the water-soluble component (e.g change of inorganic/WSOC ratio). Kim et al. (2006) have shown that the hygroscopicity of aerosol particles at Gosan was correlated with the mass fraction of sulfate. This indicates that B is mainly determined by inorganic components because hygroscopicity is mainly determined by B (e.g. Kreidenweis et al., 2005; Mochida et al., 2006). This is consistent with the present observations because the mass fraction of inorganic compounds was significantly larger than that of WSOC during this period (Fig. 8).

The D_{50} at SS=0.097% did not necessarily correlate with those of higher SSs (Fig. 4b), as discussed in Sect. 4.2.2. Correlation of D_{50} at SS=0.097% with those at higher SSs decreased with the increase in SS (r^2=0.25 and 0.00 for SS=0.27% and 0.97%, respectively). This indicates that the temporal variation of the mass fraction of $PM_{2.5}$ was reflected in that of D_{50} at SS=0.097% (100–200 nm) but was not reflected in D_{50} at higher SSs (<100 nm). This is because the contribution to the $PM_{2.5}$ mass concentration of particles with diameters smaller than 100 nm was much smaller than that of 100–200 nm.

Table 3. Average concentration of inorganic components during the observation period.

NH_4^+	Na^+	K^+	Ca^{2+}	Mg^{2+}	NO_3^-	SO_4^{2-}	Cl^-
1.57 (μg/m^3)	0.38	0.26	0.43	0.18	1.44	3.96	0.49

5.2 Comparison of D_{50} and calculated D_{crit}

In this section, we compare the observed D_{50} and the D_{crit} calculated from the simultaneously measured chemical composition. We first discuss the assumptions used to calculate A and B in Köhler theory (Sect. 2). The surface tension of water (72 mN/m) was assumed for the calculation of A. The calculation was performed at T=300 K. For the calculation of B, the ideal solution approximation (ϕ=1) was used. We used the simultaneously measured aerosol chemical composition ($PM_{2.5}$) assuming that chemical composition was not size-dependent. Assumptions regarding the chemical composition and chemical properties of organic compounds (e.g. molecular weight (MW), elemental ratio, density) are also required for the calculation of B. Kawamura et al. (2003) and Mochida et al. (2003) measured dicarboxylic acids and other water-soluble organic compounds over the Sea of Japan and Yellow Sea during the ACE-Asia campaign. The concentration of oxalic acid was higher than that of other compounds by an order of magnitude. Simoneit et al. (2004) also measured dicarboxylic acids at Gosan during the ACE-Asia campaign. Adipic acid was the largest-MW linear molecule among the dicarboxylic acids they measured. Oxalic acid has one of the smallest molecular weights among atmospheric aerosol organic compounds. Therefore, if we assume that all carbon atoms in WSOC originated from oxalic acid, we will estimate a maximum Raoult's effect. In this study, this assumption is called as "oxalic acid assumption". As an extreme case, we calculated D_{crit} using this assumption. The average molecular weight of WSOC should be higher than that of oxalic acid because dicarboxylic acids and saccharides with larger molecular weights were also observed at Gosan (Simoneit et al., 2004). In fact, Miyazaki et al. (2007) indicated that a significant portion of WSOC measured during the ABC-EAREX2005 campaign could be attributed to organic compounds having a MW larger than oxalic acid. To test the sensitivity of D_{crit} to the assumed WSOC composition, we also calculated D_{crit} assuming that the average properties (MW, elemental composition, and density) of water-soluble organic compounds are equal to those of adipic acid. In this study, this assumption is called the "adipic acid assumption", although this does not mean that all WSOC originated from adipic acid. In addition, recent studies have shown that significant fractions (20–60%) of WSOC are high-molecular weight compounds such as humic-like substances (HULIS) (Graber and Rudich, 2006, and references therein). Calculating D_{crit} under the assumption that all WSOC originated from HULIS (HULIS assumption) corresponds to the lowest estimate of Raoult's effect. As in other cases, we need the chemical properties of HULIS for the calculation, although chemical properties of HULIS vary depending on the samples used (Graber and Rudich, 2006). For this calculation, we assumed an elemental composition of HULIS of C: H: O=1: 1.16: 0.63 (Dinar et al., 2006a), a density of 1.5 g/cm^3 (Dinar et al., 2006b; Hoffer et al., 2006), and an average molecular weight of 700 Da (Dinar et al., 2006a). In these calculations, water-soluble organic compounds were assumed to be completely dissolved in water (ε=1).

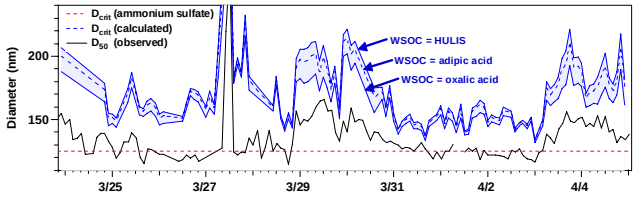

Fig. 9. Comparison of observed D_{50} and calculated D_{crit} at SS=0.097%. The upper and lower blue lines were calculated using the "HULIS assumption" and "oxalic acid assumption", respectively. See text for details of the calculations.

The chemical properties of WIOC are also required for the calculation of B. Simoneit et al. (2004) have measured alkanes, fatty acids, and polycyclic aromatic hydrocarbons (PAHs) at Gosan. Among these compounds, the mass fractions of PAHs were very limited. Most of the carbon atoms of alkanes and fatty acids are in methylene groups ($-CH_2-$). Therefore, we assumed that all carbon atoms in WIOC originated from methylene groups. The density of WIOC was assumed to be 0.8 g/cm^3 because the densities of hydrocarbons and fatty acids are typically 0.7–0.9 g/cm^3 (Pang et al., 2006). The properties of EC were assumed to be equal to those of graphite. The values used for the calculation are summarized in Table 4.

The observed D_{50} and calculated D_{crit} at SS=0.097% are compared in Fig. 9. This figure shows three calculated results based on the oxalic acid, adipic acid, and HULIS assumptions. In all cases, the temporal variations of the calculated D_{crit} correlate with the observed D_{50}. However, the calculated D_{crit} values are systematically larger than the observations by 20–29%.

The correlations of D_{50} and the calculated D_{crit} (adipic acid assumption) are shown in Fig. 10. At all SSs, the

Table 4. Values used for the calculation of D_{crit}. υ for WIOC and EC are not shown here because they are insoluble in water.

	Assumed composition	Molecular weight(MW)	υ	ρ(g/cm^3)
Ammonium sulfate	$(NH_4)_2SO_4$	132.14	3	1.77
Ammonium nitrate	NH_4NO_3	80.04	2	1.72
WSOC (oxalic acid)	$(COOH)_2$	90.04	1	1.9
WSOC (adipic acid)	$HOOC(CH_2)_4COOH$	146.14	1	1.36
WSOC (HULIS)	$CH_{1.16}O_{0.63}$	700	1	1.5
WIOC	$(-CH_2-)$	14/carbon atom	N/A	0.8
EC	C (graphite)	12/carbon atom	N/A	2.0

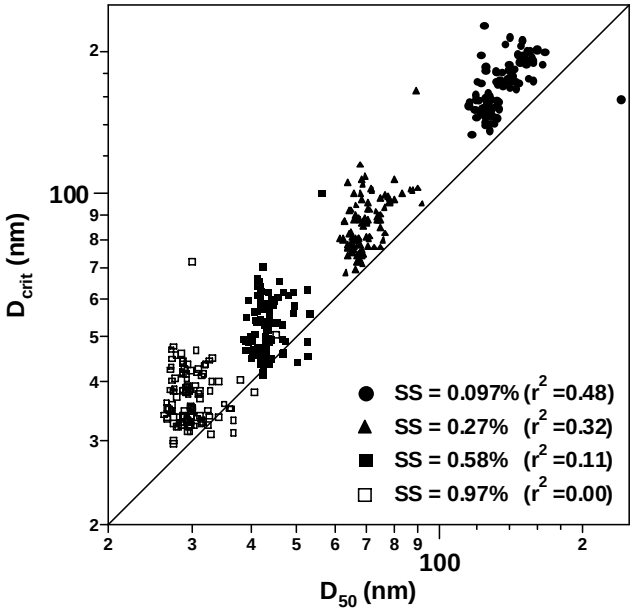

Fig. 10. Scatter plot of D_{50} (observed) and calculated D_{crit} (calculated). The adipic acid assumption was used for the calculation shown in this figure.

calculated diameters are larger than the observations. The differences between the calculated D_{crit} and the observed D_{50} (calc–obs) are summarized in Table 5. In all cases, D_{crit} was overestimated by 16–29%.

The r^2 values decrease with increasing SS (diminishing D_{50}). This is likely due to the size dependence of the temporal variation of the aerosol chemical composition, as discussed in Sect. 4.2.2.

5.3 Possible causes of the discrepancy

In this section, we discuss the possible causes of the difference between D_{50} and D_{crit} and identify critical assumptions for the calculation of D_{crit}.

In calculating B, we assumed the composition and chemical properties of each component. The average chemical properties of water-soluble organic compounds were assumed to be identical to those of oxalic acid, adipic acid, or HULIS. Nevertheless, the D_{crit} values were larger than D_{50} even in the case of the oxalic acid assumption (the maximum estimation of B). Therefore, the assumption of the chemical composition of WSOC is not the main cause of this discrepancy.

We assumed a density of 0.8 g/cm^3 for water-insoluble organic compounds. If the actual density were larger than this value, this would lead to the overestimation of D_{crit} because of the underestimation of B (Eq. 1). However, a sensitivity study of the density of WIOC (up to 1.2 g/cm^3) under the oxalic acid assumption showed that calculated D_{crit} still overestimated the observations (D_{crit}–D_{50}=20±12 nm at SS=0.097%).

The assumption of complete dissolution corresponds to the upper limit in estimated B, and therefore the lower limit of D_{crit}. For instance, Huff Hartz et al. (2006) showed that the D_{crit} of slightly soluble organic compounds calculated using the complete dissolution assumption is smaller than D_{crit} calculated assuming limited solubility. We used the ideal solution approximation in the calculation. If the discrepancy is due to this effect, the osmotic coefficient at the critical droplet diameters needs to be increased by a factor of about 2, considering the magnitude of the discrepancy (Table 5) and Eq. (2). Nevertheless, such a large change in the osmotic coefficient is unlikely, as the solution was very dilute at the critical droplet diameters.

In this study, the aerosol chemical composition was measured at $PM_{2.5}$. If the chemical compositions of $PM_{2.5}$ do not represent those at D_{50} (<200 nm), it causes an error in the calculation of D_{crit}. We discuss this point in detail in Sect. 5.3.1.

The surface tension of water was assumed for the calculation of A in Eq. (2). If the decrease in surface tension due to WSOC was significant, it may affect the D_{crit} (Facchini et al., 1999). This point is discussed in Sect. 5.3.2.

Table 5. Differences between D_{50} (observed) and calculated D_{crit} (D_{crit}−D_{50}). The values in parentheses show the magnitude of the difference in %. "Oxalic acid", "adipic acid", and "HULIS" show the oxalic acid, adipic acid, and HULIS assumptions, respectively.

	SS=0.097%	0.27%	0.58%	0.97%
Oxalic acid	27±18(nm) (20±12%)	13±10 (18±13%)	7 ± 7 (16±15%)	6±6 (21±19%)
Adipic acid	34±19 (26±13%)	17±11 (24±15%)	9±8 (22±17%)	8±6 (27±22%)
HULIS	39±20 (29±14%)	17±12 (25±16%)	10±8 (23±18%)	8±7 (26±23%)

5.3.1 Size dependence of chemical composition

Some studies have used size-resolved aerosol chemical composition for CCN closure studies (e.g. Cantrell et al., 2001; Roberts et al., 2002). These studies have shown the size-dependence of aerosol chemical composition. In addition, Medina et al. (2007) have shown that the use of size-resolved chemical composition can decrease the error in the closure of the CCN number concentration. Topping et al. (2004) measured size-resolved chemical composition at Gosan during the ACE-Asia campaign using a Berner impactor. They reported the size distribution of mass fractions of inorganic compounds and WSOC, and the results clearly showed the size-dependence. However, it is difficult to use their results to estimate the effect of size dependent chemical composition because they did not measure water-insoluble components of the impactor samples. Mochida et al. (2007) measured aerosol chemical compounds sampled with a Micro-Orifice Uniform Deposit Impactor (MOUDI) over the East China Sea and the Sea of Japan during the ACE-Asia campaign. They found that the submicron mode was enriched by non-sea salt (nss)-SO_4^{2-} ([OC]/[nss-SO_4^{2-}]≈0.2 at 0.18–0.56 μm), whereas the supermicron mode was enriched by organic compounds ([OC]/[nss-SO_4^{2-}]≈1 at 1.8–5.6 μm). The median value of [OC]/[SO_4^{2-}] in the present study is 1.0, suggesting that $PM_{2.5}$ chemical composition was affected by super-micron particles by comparison with the ratio of Mochida et al. (2007).

The D_{crit} for each SS was calculated using the chemical composition of the sub-micron mode particle given in Table 2 in Mochida et al. (2007) assuming that OC was entirely composed of WIOC, because the fraction of WSOC was much smaller than that of WIOC (Fig. 8), and WSOC concentration was not reported. The major difference of this calculation is the higher sulfate fraction ([OC]/[nss-SO_4^{2-}]≈0.2). At SS=0.097%, the observed D_{50} was 136±17 nm, and the calculated D_{crit} using the data of Mochida et al. (2007) was 142 nm, as summarized in Fig. 11. In the case of other SSs, D_{crit} also agrees with the average value of D_{50}. This result shows possible effects of the size-dependent chemical composition on CCN activation.

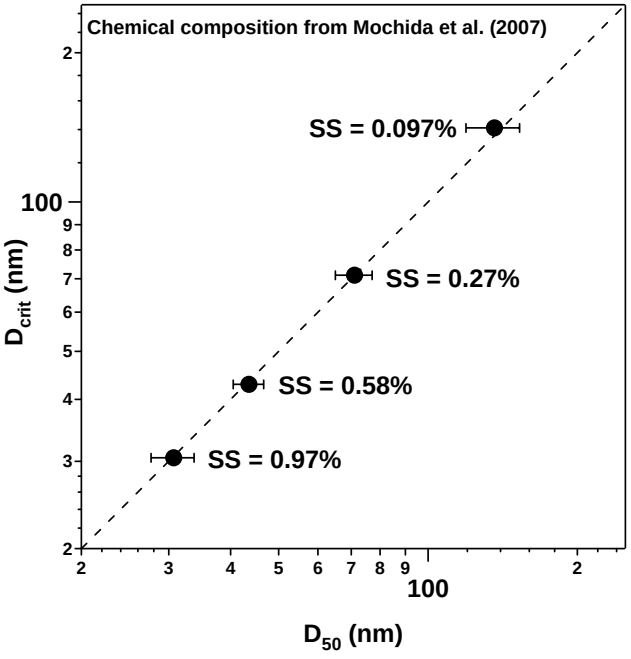

Fig. 11. Comparison of measured D_{50} and D_{crit} calculated using the chemical composition of Mochida et al. (2007). See the text for detailed explanation.

The size dependence of aerosol chemical composition is clearer for the period of new particle formation. The D_{50} values of newly formed particles were very close to that of ammonium sulfate, indicating that particles were predominantly composed of inorganic compounds at the time (Sect. 4.2.3.). In particular, newly formed particles grew larger than D_{50} at SS=0.097% on 31 March (Fig. 4), and D_{50} values were nearly equal to the D_{crit} of ammonium sulfate on that day (Fig. 9). However, the mass fraction of carbonaceous aerosols (WSOC+WIOC+EC) at $PM_{2.5}$ was about 30% at this time (Fig. 8), and this led to the overestimation of D_{crit}

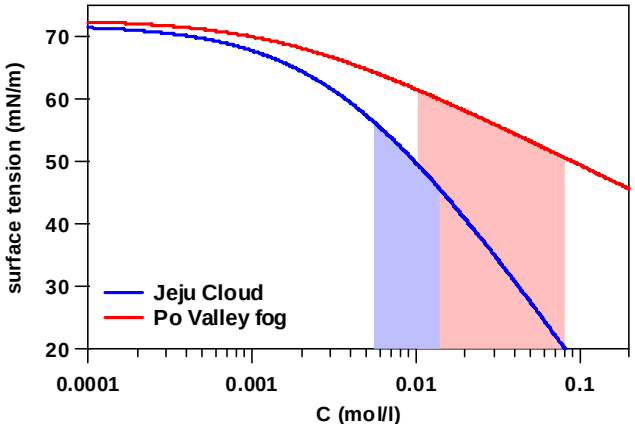

Fig. 12. Decrease of surface tension calculated using the parameters for Jeju cloud water and Po Valley fog by McFiggans et al. (2006). The colored area in the figure corresponds to the values at the critical SSs.

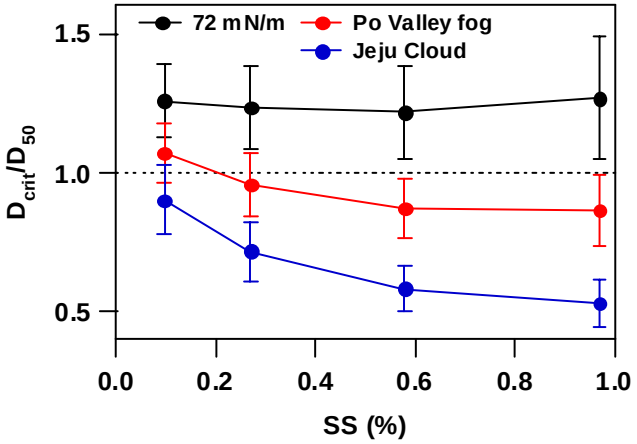

Fig. 13. Comparison of D_{crit}/D_{50} calculated using several surface tension parameters. The calculation was performed using the adipic acid approximation.

(Fig. 9). The decrease of D_{50} associated with new/secondary particle formation was also observed on 25 March. In this case, the mass fraction of water-insoluble compounds was also 30–40%, and this caused the overestimation of D_{crit}. These results suggest that the $PM_{2.5}$ mass concentration was biased by large (>200-nm) particles, at least during these periods.

5.3.2 Decrease of surface tension by organic compounds

As described above, the surface tension of water was assumed for the calculation in this study. Nevertheless, if the decrease in surface tension due to organic compounds was significant, it may affect the critical SS of the particles (Facchini et al. 1999). Surface tension lowering effects have been observed in various regions of the world such as Po Valley in Italy (Facchini et al. 1999), Mace Head in Ireland (Cavalli et al. 1999), and the Great Hungarian Plain (Kiss et al. 2005. In particular, Decesari et al. (2005) measured the surface tension lowering effect of aerosol, cloud water, and wet deposition samples at Jeju Island during the ACE-Asia campaign. They showed that the decrease of the surface tension due to aerosol was relatively small, whereas the surface tension decrease of cloud water and wet-deposition samples was significant. McFiggans et al. (2006) compared these results, and they showed that the magnitude of the effect for cloud water at Jeju Island was the most significant, and the effects for Po Valley and Mace Head samples were not as large as that of cloud water at Jeju (the red and blue lines in Fig. 12).

They summarized the fitted parameters of the Szyszkowski-Langmuir Eq. (3) obtained for these observation results,

$$\sigma = \sigma_0 - bT\ln(1 + aC) \quad (3)$$

where σ_0 is the surface tension of pure water, C is the WSOC concentration of the solution, and a and b are the empirical parameters obtained by fitting the observational results. In order to investigate the sensitivity of D_{crit} to surface tension, we calculated D_{crit} at each SS using the parameters given by McFiggans et al. (2006). In this calculation, the adipic acid assumption was used, and the values for Jeju cloud water and Po Valley fog were employed. Substituting σ in Eq. (1) by that expressed by Eq. (3), the D_{crit} values were obtained by numerical calculation. The results are summarized in Fig. 13. In the case of Jeju cloud water, the calculated diameters for all SSs are smaller than the observed D_{50} by 10–47%, and the use of the equation for Po Valley decreased the differences between D_{crit} and D_{50} (7 to −13%). This indicates that the decrease of surface tension can potentially explain the discrepancy. The surface tension at the critical SS was about 46–56 mN/m (Jeju cloud water) and 51–62 mN/m (Po Valley), respectively (Fig. 12).

The discussion in this section and Sect. 5.3.1 shows that the size- dependence of chemical composition and the decrease in surface tension are the critical parameters in estimating D_{crit}. For a more quantitative assessment of these effects, we need simultaneous measurements of these parameters and D_{50}.

5.4 Impact of D_{crit} on CCN number concentration

The main purpose of the calculation of D_{crit} is the precise estimation of CCN number concentration from the particle size distribution. We estimated the difference in CCN number concentration due to the difference in D_{50} and calculated D_{crit}. The following equation was used for the assessment of

the difference:

$$\frac{\Delta N_{\mathrm{CCN}}}{N_{\mathrm{CCN}}} = -\frac{\int_{\log(D_{50})}^{\log(D_{\mathrm{crit}})} f_N(\log D_p) d\log D_p}{N_{\mathrm{CCN}}} \quad (4)$$

where N_{CCN} is the number concentration of CCN measured by the CCN counter, ΔN_{CCN} is the difference of the CCN number concentration caused by the error in the estimation of D_{crit}, and $f_N(\log D_p)$ is the number size distribution measured by the SMPS. Therefore, $\Delta N_{\mathrm{CCN}}/N_{\mathrm{CCN}}$ is the ratio of the difference of the CCN number concentration due to the difference in D_{crit} and the observed CCN number concentration. $\Delta N_{\mathrm{CCN}}/N_{\mathrm{CCN}}$ depends on the number size distribution ($f_N(\log D_p)$) and the uncertainty of the chemical composition (D_{crit}–D_{50}). For this calculation, the calculated D_{crit} (adipic acid assumption, surface tension of water) was used. In addition to the adipic acid assumption, we also calculated $\Delta N_{\mathrm{CCN}}/N_{\mathrm{CCN}}$ using the ammonium sulfate assumption (D_{crit}=D_{crit} of ammonium sulfate) because this assumption has frequently been used in previous CCN studies (e.g. VanReken et al., 2003), including those for Gosan (Yum et al., 2007). The results are summarized in Fig. 14. In general, the adipic acid approximation underestimates the CCN number concentration due to the overestimation of D_{crit}, whereas the ammonium sulfate approximation overestimates the CCN number concentration because of the underestimation of the D_{crit}. At SS=0.097%, $\Delta N_{\mathrm{CCN}}/N_{\mathrm{CCN}}$ was -0.27 ± 0.14 and 0.16 ± 0.18 for the adipic acid and ammonium sulfate approximations, respectively. These values give a measure of the uncertainty associated with the CCN prediction based on the results of this study. The absolute value of $\Delta N_{\mathrm{CCN}}/N_{\mathrm{CCN}}$ increased with decreasing SS. During the observation period, the average values of B did not show a significant dependence on the value of SS as discussed in Sect. 4.2.2, and the magnitude of the error associated with the estimation of D_{crit}did not depend on SS significantly. Thus, this trend was not mainly due to the size dependence of the chemical composition. D_{crit} decreased with increasing SS. The particle number concentration between D_{50} and D_{crit} was smaller at higher SS in comparison with the CCN number concentration because at higher SS a larger fraction of CCN is in the size range larger than D_{50}, as can be seen from Fig. 6. These results show that the effect of chemical composition on N_{CCN} was more important at lower SS, and the aerosol number size distribution was important at higher SS.

6 Summary

We measured the CCN number concentration (N_{CCN}) and the size-resolved CCN/CN ratios at SS=0.097, 0.27, 0.58, and 0.97% on Jeju Island, Korea, during 18 March–5 April 2005. The average CCN number concentrations for the whole observational period were as high as $1194\pm746\,\mathrm{cm}^{-3}$ (SS=0.097%) and $3966\pm1686\,\mathrm{cm}^{-3}$ (SS=0.97%). The CCN/CN ratios monotonically increased with increasing particle diameter, and the diameter at CCN/CN=0.5 was defined as D_{50}. The average D_{50} values at SS=0.097% and 0.97 % were 136 nm and 31 nm, respectively. These values were slightly larger than those of ammonium sulfate particles (125 and 27 nm at SS=0.097% and 0.97%, respectively). In particular, D_{50} diameters of newly formed particles and those of ammonium sulfate particles were almost identical for SS=0.97, 0.58 and 0.27%, indicating that these particles were mainly composed of ammonium sulfate. The peak diameter of the CCN size distribution averaged for the whole observational period was about 150 nm at SS=0.097% and shifted to about 80 nm at SS=0.97%.

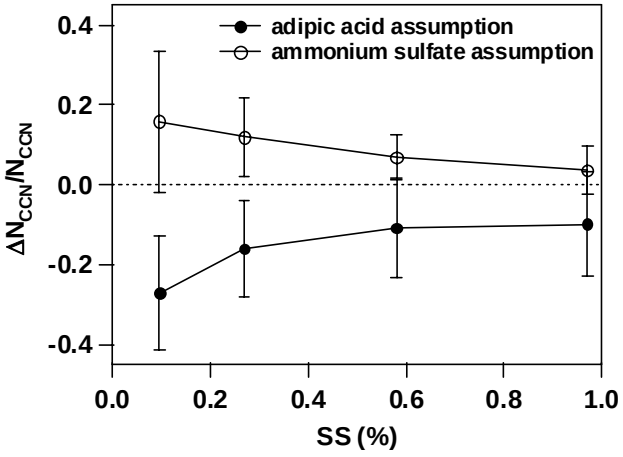

Fig. 14. Average values and standard deviations of $\Delta N_{\mathrm{CCN}}/N_{\mathrm{CCN}}$.

The temporal variation of D_{50} at SS=0.097% was negatively correlated with the variation of the water-soluble fraction (inorganics + WSOC) of the aerosol components. For quantitative comparison, the threshold diameters for CCN activation (D_{crit}) were calculated by Köhler theory assuming the surface tension of water and $PM_{2.5}$ aerosol chemical composition. The calculated D_{crit} values were correlated with D_{50} at SS=0.097% (r^2=0.48). However, D_{crit} was systematically larger than D_{50} by about 16–29%. Sensitivity studies have shown that this discrepancy can be explained by possible differences in aerosol chemical composition between the sub-micron and super-micron size ranges. In addition, a decrease of the surface tension due to the existence of WSOC can also significantly decrease D_{crit}.

The particle number concentrations in the size range between D_{50} and D_{crit}(ΔN_{CCN}) were calculated using the observed size distribution. The ratios of ΔN_{CCN} to N_{CCN} ($\Delta N_{\mathrm{CCN}}/N_{\mathrm{CCN}}$) were estimated to be -0.27 ± 0.14 and -0.10 ± 0.13 at SS=0.097% and 0.97%, respectively, assuming that water-soluble organic compounds are represented by adipic acid. The $\Delta N_{\mathrm{CCN}}/N_{\mathrm{CCN}}$ ratio gives a measure of the uncertainty in estimating CCN number concentrations using

particle number size distributions and $PM_{2.5}$ chemical compositions in the East Asia region.

Acknowledgements. We acknowledge anonymous reviewers for their useful comments. We also thank C. S. Hong and Y. J. Kim for their support of the observations. This work was supported by the Ministry of Education, Culture, Sports, Science, and Technology (MEXT), the Japanese Science and Technology Agency (JST), and the global environment research fund of the Japanese Ministry of the Environment. M. Kuwata thanks the Japan Society for the Promotion of Science (JSPS) for a JSPS Research Fellowship for Young Scientists. J. H. Kim and S. S. Yum were supported by the Korean Ministry of Environment under the "Eco-techonopia 21 project".

Edited by: C. Chan

References

Akimoto, H.: Global air quality and pollution, Science, 302, 1716–1719, 2003.

Arnold, F.: Atmospheric aerosol and cloud condensation nuclei formation: A possible influence of cosmic rays?, Space. Sci. Reviews, 125, 169–186, 2006.

Bae, M.-S., Schauer, J. J., DeMinter, J. T., Turner, J. R., Smith D., and Cary, R. A.: Validation of a semi-continuous instrument for elemental carbon and organic carbon using a thermal-optical method, Atmos. Environ., 38, 2885–2893, 2004.

Buzorius, G., McNaughton, C. S., Clarke, A. D., Covert, D. S., Blomquist, B., Nielsen, K., and Brechtel, F. J.: Secondary aerosol formation in continental outflow conditions during ACE-Asia, J. Geophys. Res., 109, D24203, doi:10.1029/2004JD004749, 2004.

Cantrell, W., Shaw, G., Cass, G. R., Chowdhury, Z., Hughes, L. S., Prather, K. A., Guazzotti, S. A., and Coffee, K. R.: Closure between aerosol particles and cloud condensation nuclei at Kaashidhoo Climate Observatory, J. Geophys. Res., 106(D22), 28 711–28 718, 2001.

Carmichael, G. R., Hong, M., Ueda, H., Chen, L., Murano, K., Park, J. K., Lee, H., Kim, Y., Kang, C., and Shim, S.: Aerosol composition at Cheju Island, Korea, J. Geophys. Res., 102(D5), 6047–6062, 1997.

Cavalli, F., Facchini, M. C., Decesari, S., et al.: Advances in characterization of size-resolved organic matter in marine aerosol over the North Atlantic, J. Geophys. Res., 109, D24215, doi:10.1029/2004JD005137, 2004.

Chameides, W. L., Luo, C., Saylor, R., Streets, D. G., Huang, Y., Bergin, M., and Giorgi, F.: Correlation between model-calculated anthropogenic aerosols and satellite-derived cloud optical depths: Indication of indirect effect?, J. Geophys. Res., 107(D10), 4085, doi:10.1029/2000JD000208, 2002.

Clegg, S. L., Rard, J. A., and Pitzer, K. S.: Thermodynamic properties of 0-6 mol Kg-1 aqueous sulfuric acid from 273.15K to 328.15K, J. Chem. Soc. Faraday Trans., 90, 1875–1894, 1994.

Clegg, S. L., Milioto S., and Palmer, D. A.: Osmotic and activity coefficients of aqueous $(NH_4)_2SO_4$ as a function of temperature, and $(NH_4)_2SO_4$ - H_2SO_4 mixtures at 298.15 K and 323.15 K, J. Chem. Eng. Data, 41, 455–467, 1996.

Corrigan, C. E. and Novakov, T.: Cloud condensation nucleus activity of organic compounds: A laboratory study, Atmos. Environ., 33, 2661–2668, 1999.

Covert, D. S., Gras, J. L., Wiedensohler A., and Stratmann, F.: Comparison of directly measured CCN with CCN modeled from the number-size distribution in the marine boundary layer during ACE 1 at Cape Grim, Tasmania, J. Geophys. Res., 103(D13), 16 597–16 608, 1998.

Cruz, C. N. and Pandis, S. N.: Deliquescence and hygroscopic growth of mixed inorganic-organic atmospheric aerosol, Environ. Sci. Technol., 34, 4313–4319, 2000.

Decesari, S., Facchini, M. C., Fuzzi, S., McFiggans, G. B., Coe, H., and Bower, K. N.: The water-soluble organic component of size-segregated aerosol, cloud water and wet depositions from Jeju Island during ACE-Asia, Atmos. Environ., 39, 211–222, 2005.

Dinar, E., Taraniuk, I., Graber, E. R., Katsman, S., Moise, T., Anttila, T., Mentel, T. F., and Rudich, Y.: Cloud Condensation Nuclei properties of model and atmospheric HULIS, Atmos. Chem. Phys., 6, 2465–2481, 2006a, http://www.atmos-chem-phys.net/6/2465/2006/.

Dinar, E., Mentel, T. F., and Rudich, Y.: The density of humic acids and humic like substances (HULIS) from fresh and aged wood burning and pollution aerosol particles, Atmos. Chem. Phys., 6, 5213–5224, 2006b, http://www.atmos-chem-phys.net/6/5213/2006/.

Dusek, U., Frank, G. P., Hildebrandt, L., Curtius, J., Schneider, J., Walter, S., Chand, D., Drewnick, F., Hings, S., Jung, D., Borrmann, S., and Andreae, M. O.: Size matters more than chemistry for cloud-nucleating ability of aerosol particles, Science, 312, 1375–1378, 2006.

Facchini, M. C., Mircea, M., Fuzzi, S., and Charlson, R. J.: Cloud albedo enhancement by surface-active organic solutes in growing droplets, Nature, 401, 257–259, 1999.

Grabber, E. R. and Rudich Y: Atmospheric HULIS: How humic-like are they? A comprehensive and critical review, Atmos. Chem. Phys., 6, 729–753, 2006, http://www.atmos-chem-phys.net/6/729/2006/.

Hoffer, A., Gelencsèr, A., Guyon, P., Kiss, G.., Schmid, O., Frank, G. P., Artaxo, P., and Andrea, M. O.: Optical properties of humic-like substances (HULIS) in biomass-burning aerosols, Atmos. Chem. Phys., 6, 3563–3570, 2006, http://www.atmos-chem-phys.net/6/3563/2006/.

Hudson, J. G. and Yum, S. S.: Cloud condensation nuclei spectra and polluted and clean clouds over the Indian Ocean, J. Geophys. Res., 107(D19), 8022, doi:10.1029/2001JD000829, 2002.

Huff Hartz, K. F., Tischuk, J. E., Chan, M. N., Chan, C. K., Donahue, N. M., and Pandis, S. N.: Cloud condensation nuclei activation of limited solubility organic aerosol, Atmos. Environ., 40, 605–617, 2006.

Kawamoto, K., Hayasaka, T., Uno, I., and Ohara, T.: A correlative study on the relationship between modeled anthropogenic aerosol concentration and satellite-observed cloud properties over east Asia, J. Geophys. Res., 111, D19201, doi:10.1029/2005JD006919, 2006.

Kawamura, K., Umemoto, N., Mochida, M., Bertram, T., Howell, S., and Huebert, B. J.: Water-soluble dicarboxylic acids in the tropospheric aerosols collected over east Asia and western North Pacific by ACE-Asia C-130 aircraft, J. Geophys. Res., 108(D23), 8639, doi:10.1029/2002JD003256, 2003.

Kim, J., Yoon, S.-C., Jefferson, A., and Kim, S.-W.: Aerosol hygroscopic properties during Asian dust pollution, and biomass burning episodes at Gosan, Korea in April 2001, Atmos. Environ., 40, 1550–1560, 2006.

Kiss, G., Tombàcz, E., and Hanson, H.-C.: Surface tension effects of Humic-like substances in the aqueous extract of tropospheric fine aerosol, J. Atmos. Chem., 50, 279–294, 2005.

Knutson, E. O. and Whitby, K. T.: Aerosol classification by electric mobility: Apparatus, theory, and applications, J. Aerosol. Sci., 6, 443–451, 1975.

Kondo, Y., Komazaki, Y., Miyazaki, Y., et al.: Temporal variations of elemental carbon in Tokyo, J. Geophys. Res., 111, D12205, doi:10.1029/2005JD006257, 2006.

Kondo, Y., Miyazaki, Y., Takegawa, N., Miyakawa, T., Weber, R. J., Jimenez, J. L., Zhang, Q., and Worsnop, D. R.: Oxygenated and water-soluble organic aerosols in Tokyo, J. Geophys. Res., 112, D01203, doi:10.1029/2006JD007056, 2007.

Kreidenweis, S. M., Koehler, K., DeMott, P. J., Prenni, A. J., Carrico, C., and Ervens, B.: Water activity and activation diameters from hygroscopicity data – Part I: Theory and application to inorganic salts, Atmos. Chem. Phys., 5, 1357–1370, 2005

Kuwata, M., Kondo, Y., Mochida, M., Takegawa, N., and Kawamura, K.: Dependence of CCN activity of less volatile particles on the amount of coating observed in Tokyo, J. Geophys. Res., 112, D11207, doi:10.1029/2006JD007758, 2007.

Laaksonen, A., Hamed, A., Joutsensaari, J., Hiltunen, L., Cavalli, F., Junkermann, W., Asmi, A., Fuzzi, S., and Facchini, M. C.: Cloud condensation nucleus production from nucleation events at a highly polluted region, Geophys. Res. Lett., 32, L06812, doi:10.1029/2004GL022092, 2005.

Lee, J. Y., Kim, Y. P., Kang, C.-H., Ghim, Y. S., and Kaneyasu, N.: Temporal trend and long-range transport of particulate polycyclic aromatic hydrocarbons at Gosan in northeast Asia between 2001 and 2004, J. Geophys. Res., 111, D11303, doi:10.1029/2005JD006537, 2006.

Lohmann, U. and Feichter, J.: Global indirect aerosol effects: A review, Atmos. Chem. Phys., 5, 715–737, 2005, http://www.atmos-chem-phys.net/5/715/2005/.

Markowski, G. R.: Improving Twomey's algorithm for inversion of aerosol measurement data, Aerosol. Sci. Technol., 7, 127–141, 1987.

McFiggans, G.,Artaxo, P., Baltensperger, U., et al.: The effect of physical and chemical aerosol properties on warm cloud droplet activation, Atmos. Chem. Phys., 6, 2593–2649, 2006, http://www.atmos-chem-phys.net/6/2593/2006/.

Matsumoto, K., Tanaka, H., Nagao, I., and Ishizaka, Y.: Contribution of particulate sulfate and organic carbon to cloud condensation nuclei in the marine atmosphere, Geophys. Res. Lett., 24(6), 655–658, 1997.

Medina, J., Nenes, A., Sotiropoulou, R.-E. P., Cottrell, L. D., Ziemba, L. D., Beckman, P. J, and Griffin, R. J.: Cloud condensation nuclei closure during the International Consortium for Atmospheric Research on Transport and Transformation 2004 campaign: Effects of size-resolved composition, J. Geophys. Res., 112, D10S31, doi:10.1029/2006JD007588, 2007.

Miyazaki, Y., Kondo, Y., Takegawa, N., Komazaki, Y., Fukuda, M., Kawamura, K., Mochida, M., Okuzawa, K., and Weber, R. J.: Time-resolved measurements of water-soluble organic carbon in Tokyo, J. Geophys. Res., 111, D23206, doi:10.1029/2006JD007125, 2006.

Miyazaki, Y., Kondo, Y., Kodama, D., Han, S., Koike, M., Komazaki, Y., Tanimoto, H., and Matsueda, H.: Chemical characteristics of water-soluble organic carbon in the Asian outflow, J. Geophys. Res., 112, D22S30, doi:10.1029/2007JD009116,2007.

Mochida, M., Kawamura, K., Umemoto, N., Kobayashi, M., Matsunaga, S., Lim, H., Turpin, B. J., Bates, T. S., and Simoneit, B. R. T.: Spatial distributions of oxygenated organic compounds (dicarboxylic acids, fatty acids, and levoglucosan) in marine aerosols over the western Pacific and off the coast of East Asia: Continental outflow of organic aerosols during the ACE-Asia campaign, J. Geophys. Res., 108(D23), 8638, doi:10.1029/2002JD003249, 2003.

Mochida, M., Kuwata, M., Miyakawa, T., Takegawa, N., Kawamura, K., and Kondo, Y.: Relationship between hygroscopicity and cloud condensation nuclei activity for urban aerosols in Tokyo, J. Geophys. Res., 111, D23204, doi:10.1029/2005JD006980, 2006.

Mochida, M., Umemoto, N., Kawamura, K., Lim, H.-J., and Turpin, B. J.: Bimodal size distributions of various organic acids and fatty acids in the marine atmosphere: Influence of anthropogenic aerosols, Asian dusts, and sea spray off the coast of East Asia, J. Geophys. Res., 112, D15209, doi:10.1029/2006JD007773, 2007.

O'Dowd, C. D., Hmeri, K., Mkel, J. M., et al.: A dedicated study of New Particle Formation and Fate in the Coastal Environment (PARFORCE): Overview of objectives and achievements, J. Geophys. Res., 107(D19), 8108, doi:10.1029/2001JD000555, 2002.

Orsini, D. A., Ma, Y., Sullivan, A., Sierau, B., Baumann, K., and Weber, R. J.: Refinements to the particle–into-liquid sampler (PILS) for ground and airborne measurements of water soluble aerosol composition, Atmos. Environ., 37, 1243–1259, 2003.

Pang Y., Turpin, B. J., and Gundel, L. A.: On the importance of organic oxygen for understanding organic aerosol particles, Aerosol. Sci . Technol., 40, 128–133, 2006.

Raymond, T. M. and Pandis, S. N.: Cloud activation of single-component organic aerosol particles, J. Geophys. Res., 107(D24), 4787, doi:10.1029/2002JD002159, 2002.

Reade, L., Jennings, S. G., and McSweeney, G.: Cloud condensation nuclei measurements at Mace Head, Ireland, over the period 1994–2002, Atmos. Res., 82, 610–621, 2006.

Richter, A., Burrows, J. P., Nüb, C. Grainer, and Niemeier, U: Increase in tropospheric nitrogen dioxide over China observed from space, Nature, 437, 129–132, 2005.

Roberts, G. C., Artaxo, P., Zhou, J., Swietlicki, E., and Andreae, M. O.: Sensitivity of CCN spectra on chemical and physical properties of aerosol: A case study from the Amazon Basin, J. Geophys. Res., 107(D20), 8070, doi:10.1029/2001JD000583, 2002.

Roberts, G. C. and Nenes, A.: A continuous-flow streamwise thermal gradient CCN chamber for atmospheric measurements, Aerosol. Sci. Technol., 39, 206–221, 2005.

Sawa, Y., Tanimoto, H., Yonemura, S., Matsueda, H., Wada, A., Taguchi, S., Hayasaka, T., Tsuruta, H., Tohjima, Y., and Mukai, H.: Widespread pollution events of carbon monoxide observed over the western North Pacific during the EAREX 2005 campaign, J. Geophys. Res., 112, D22S26, doi:10.1029/2006JD008055, 2007.

Seinfeld, J. H. and Pandis, S. N.: Atmospheric Chemistry and Physics, John Wiley and Sons, Inc., New York, 2006.

Simoneit, B. R. T., Kobayashi, M., Mochida, M., Kawamura, K., Lee, M., Lim, H.-J., Turpin, B. J., and Komazaki, Y.: Composition and major sources of organic compounds of aerosol particulate matter sampled during the ACE-Asia campaign, J. Geophys. Res., 109, D19S10, doi:10.1029/2004JD004598, 2004.

Sotiropoulou, R. E. P., Tagaris, E., Pilinis, C., Anttila, T., and Kulmala, M.: Modeling new particle formation during air pollution episodes: Impacts on aerosol and cloud condensation nuclei, Aerosol. Sci . Technol., 40, 557–572, 2006.

Streets, D. G., Tsai, N. Y., Akimoto, H., and Oka, K.: Sulfur dioxide emissions in Asia in the period 1985–1997, Atmos. Environ., 34, 4413–4424, 2000.

Sullivan, A. P., Weber, R. J., Clements, A. L., Turner, J. R., Bae, M. S., and Schauer, J. J.: A method for on-line measurement of water-soluble organic carbon in ambient aerosol particles: Results from an urban site, Geophys. Res. Lett., 31, L13105, doi:10.1029/2004GL019681, 2004.

Takegawa, N., Miyazaki, Y., Kondo, Y., Komazaki, Y., T. Miyakawa, T., Jimenez, J. L., Jayne, J. T., Worsnop, D. R., Allan, J., and Weber, R. J.: Characterization of an Aerodyne Aerosol Mass Spectrometer (AMS): Intercomparison with other aerosol instruments, Aerosol Sci. Technol., 39, 760–770, 2005.

Tanimoto, H., Sawa, Y., Matsueda, H., Wada, A., Yonemura, S., Mukai, H., Wang, T., Poon, S., Wong, A., Lee, G., Jung, J. Y., Kim, K. R., Lee, M. H., Lin, N. H., Wang, J. L., Ou-Yang, C. F, and Wu, C. F.: Evaluation of standards and methods for continuous measurements of carbon monoxide at ground-based sites in Asia, Pap. Met. Geophys., 58, 85–93, doi:10.2467/mripapers.58.85, 2007.

Topping, D., Coe, H., McFiggans, Burgess, G. R., Allan, J., Alfarra, M. R., Bower, K., Choularton, T. W., Decesari, S., and Facchini, M. C.: Aerosol chemical characteristics from sampling conducted on the Island of Jeju Korea during ACE Asia, Atmos. Environ., 38, 2111–2123, 2004.

Twomey, S.: Pollution and the planetary albedo, Atmos. Environ., 8, 1251–1256, 1974.

Van Reken, T. M., Rissman, T. A., Roberts, G. C., Varutbangkul, V., Jonsson, H. H., Flagan, R. C, and Seinfeld, J. H.: Toward aerosol/cloud condensation nuclei (CCN) closure during CRYSTAL-FACE, J. Geophys. Res., 108(D20), 4633, doi:10.1029/2003JD003582, 2003.

Yum, S. S., Hudson, J. G., Song, K. Y., and Choi, B.-C.: Springtime cloud condensation nuclei concentrations on the west coast of Korea, Geophys. Res. Lett., 32, L09814, doi:10.1029/2005GL022641, 2005.

Yum, S. S., Roberts, G., Kim, J. H., Song, K., and Kim, D.: Submicron aerosol size distributions and cloud condensation nuclei concentrations measured at Gosan, Korea during the ABC-EAREX 2005, J. Geophys. Res., 112, D22S32, doi:10.1029/2006JD008212., 2007.

Wiedensohler, A.: Technical Note. An Approximation of the bipolar charge distribution for particles in the submicron size range, J. Aerosol. Sci., 19, 387–389, 1988.